Tokamak Startup Using Point-Source dc Helicity Injection

D. J. Battaglia, M. W. Bongard, R. J. Fonck, A. J. Redd, and A. C. Sontag
Department of Engineering Physics, University of Wisconsin, 1500 Engineering Drive, Madison, Wisconsin 53706, USA
(Received 19 December 2008; published 4 June 2009)

Startup of a 0.1 MA tokamak plasma is demonstrated on the ultralow aspect ratio Pegasus Toroidal Experiment using three localized, high-current density sources mounted near the outboard midplane. The injected open field current relaxes via helicity-conserving magnetic turbulence into a tokamaklike magnetic topology where the maximum sustained plasma current is determined by helicity balance and the requirements for magnetic relaxation.

DOI: 10.1103/PhysRevLett.102.225003 PACS numbers: 52.55.Fa, 52.35.Vd, 52.55.Wq

Startup and sustainment of current in a toroidal magnetically confined plasma without induction from a central solenoid has been a long-standing challenge for fusion science and high-temperature plasma research. This challenge is especially pressing for the spherical tokamak (ST) since its low-aspect-ratio geometry requires a reduced central flux core. A general approach for addressing this issue employs the concept of magnetic helicity injection, which takes advantage of the underlying connection between magnetic topology and current drive in a confined plasma.

Helicity is a measure of the degree of linkage of the magnetic flux within a closed volume and is given by $K = \int_V \mathbf{A} \cdot \mathbf{B} d^3x$ where $\mathbf{A}$ and $\mathbf{B}$ are the magnetic vector potential and field, respectively. A tokamak plasma has finite helicity since magnetic flux generated by the driven toroidal plasma current (I_p) links the externally generated toroidal magnetic field (B_ϕ). Maintaining toroidal current in a tokamak plasma requires helicity injection to balance resistive helicity dissipation ($\dot{K}_{\rm diss} = 2 \int_V \eta \mathbf{J} \cdot \mathbf{B} d^3x$).

In the dc helicity injection approach, a current is driven along open magnetic field lines between biased electrodes at the boundary of a confined plasma. Under appropriate conditions, nonaxisymmetric magnetic turbulence and reconnection can relax the open field line currents to a lower-energy state that approximates the magnetic topology of closed, nested, toroidal flux surfaces. As shown by Taylor [1], these plasma relaxation mechanisms shed magnetic energy from the plasma while conserving the global helicity of the system over the resistive helicity dissipation time scale.

Plasma formation via dc helicity injection was demonstrated using small emissive cathodes on the CDX [2] and CCT [3] experiments. These experiments observed the relaxation of open field line current into a tokamaklike magnetic topology and a global helicity content consistent with the helicity injection and dissipation rates. However, the maximum plasma current was limited to relatively low values ($I_p \leq 6$ kA) due to impurity generation from localized cathodes at high-current densities.

The coaxial helicity injection (CHI) approach, first developed in spheromak research, overcomes this limitation using large coaxial electrodes that tolerate moderate current densities [4]. CHI experiments on the HIT-II [5] and NSTX [6] ST devices demonstrated that dc helicity injection is viable for tokamak startup. However, installing large metallic electrodes and insulating materials close to the plasma may limit the application of CHI in fusion-scale facilities.

In this Letter, we demonstrate the creation of a tokamak plasma via helicity injection using localized, high-current density plasma sources that are relatively impurity-free. The maximum toroidal current sustained by this method appears to obey simple constraints from helicity conservation, magnetic relaxation, and toroidal plasma force balance. This tokamak startup system offers the advantages that the compact electrodes can be inserted into the tokamak in a variety of geometries and can be removed from the vessel following plasma formation.

These experiments are performed on the Pegasus toroidal experiment, an ultralow aspect ratio ($A \equiv R_0/a \geq 1.15$) spherical tokamak with a maximum plasma minor radius a of 0.39 m at a major radius (R_0) of 0.45 m [7]. The toroidal field rod current ($I_{\rm TF}$) is as large as 288 kA, corresponding to a vacuum toroidal field of 0.13 T at $R_0 = 0.45$ m. The focus of the nonsolenoidal startup experiments on Pegasus is to create a tokamak plasma that can be subsequently sustained by other current drive techniques.

The Pegasus point-source dc helicity injection system consists of three small plasma guns mounted 13—27 cm below the outboard midplane and a single anode mounted 20 cm above the outboard midplane at the same toroidal location [8]. Each plasma gun consists of a gas-injected washer stack (channel length of 2 cm) that supports an arc discharge between a cathode cup and an anode washer with an outer diameter of 2 cm [9,10]. Each gun can source large current densities (≤ 0.6 kA/cm^2) with low impurity production as long as the extracted current is less than the arc current (≤ 2 kA). Under this condition, the bulk of the injected current is extracted from the plasma arc discharge rather than from electrode surfaces.

For each discharge, external coils create an initial vacuum magnetic field such that helical field lines connect the aperture of each gun to the anode. Plasma ejected from each gun follows the vacuum field, forming helical plasma filaments. The number of toroidal transits each filament completes between the gun and anode is the geometric windup (G) of the field line.

The plasma guns are biased relative to the anode ($V_{\mathrm{bias}} \leq 1500$ V), driving current along the plasma filaments (I_{inj}). Initially, the current multiplication factor ($M = I_p/I_{\mathrm{inj}}$) is equal to the geometric windup. When I_{inj} is sufficiently large, the poloidal magnetic field generated by the injected current nearly cancels the inboard vacuum vertical field. Under this condition, current and magnetic field gradients drive magnetic turbulence that relaxes the system into a lower-energy, tokamaklike state with $M > G$ while maintaining a nearly constant helicity content [11]. The new magnetic topology is referred to as tokamaklike since it resembles a tokamak plasma in a toroidally averaged sense, but a majority of the field lines may be stochastic [12].

The evolution of a plasma gun-initiated discharge is shown in Fig. 1, where I_p approaches 0.1 MA [Fig. 1(a)]. Bias voltage between the guns and anode is applied at 21 ms, driving current along open field lines [Fig. 1(b)]. (Note, the oscillations in I_{inj} are an artifact of the bias circuit power supplies and do not affect the dynamics of the discharge). Around 22.5 ms, the current multiplication M exceeds the geometric windup of 2 [Fig. 1(c)] and a tokamaklike plasma forms. I_p increases as the plasma major radius, estimated using inboard and outboard midplane magnetic sensors, decreases [Fig. 1(d)]. The maximum plasma size, current, and inverse aspect ratio ($\varepsilon = 1/A$) are achieved when the plasma edge contacts both the inner and outer limiters ($R_0 \approx 0.41$ m). The equilibrium magnetic field evolution is programmed such that the plasma achieves full size and maximum current close to the gun shutoff time at 28 ms.

After gun shutoff, the open field lines at the edge are no longer driven, and the flux surfaces rapidly heal to a quiescent tokamak equilibrium. The magnetic structure of a typical gun-driven discharge at $t = 28$ ms is reconstructed with a Grad-Shafranov equilibrium solver [13], and shown in Fig. 2. The plasma is limited on both the central column and the outboard gun and anode structure, has low internal inductance ($l_i \approx 0.3$) due to the large edge current density, and has low kinetic pressure ($\beta_t \approx 1\%$).

Gun-driven plasmas generally exhibit low-n MHD activity (typically $n = 1$) during the drive period. These modes are intermittent in many discharges, but continuous in others. The $n = 1$ mode frequencies are typically in the range of 20–60 kHz, and can slowly vary by up to a factor of 2 during the drive period. The presence of these modes is strongly correlated with the helicity injection drive, but the details of these interactions are presently under study.

After gun shutoff, the edge MHD activity is strongly reduced, reflecting the healing of the stochastic driven

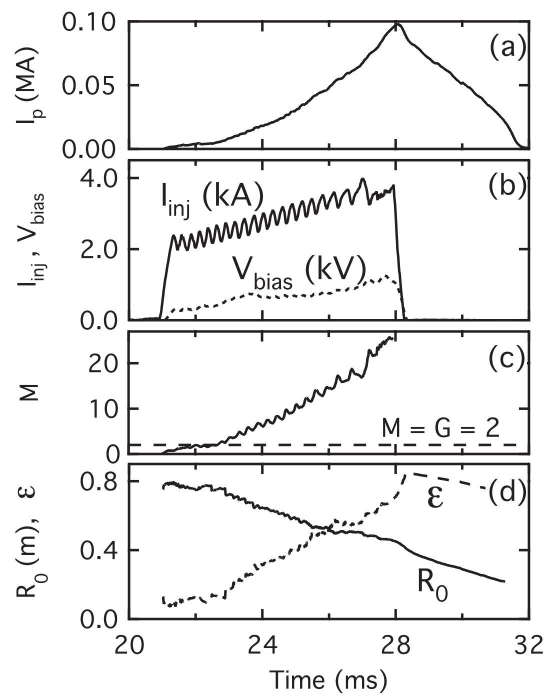

FIG. 1. Time waveforms for a typical plasma gun-initiated discharge: (a) Plasma current, (b) bias voltage and total injected current, (c) current multiplication, and (d) plasma major radius and inverse aspect ratio.

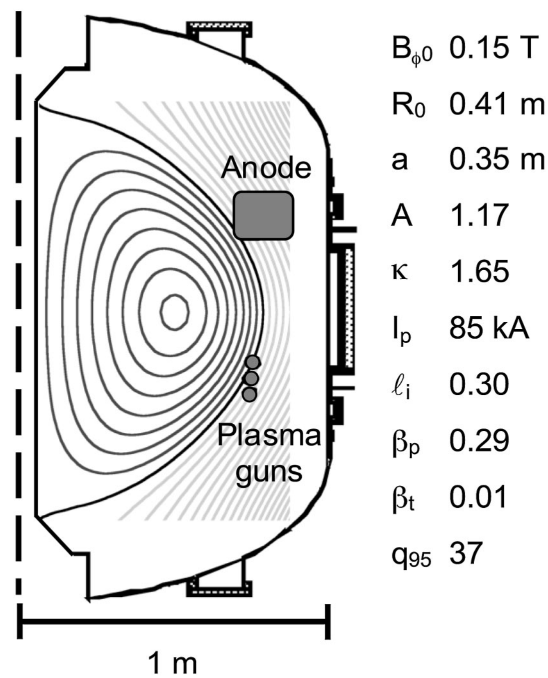

FIG. 2. Magnetic equilibrium reconstruction of poloidal flux surfaces at $t = 28$ ms.

fields into a tokamak plasma with a broad, stable current profile. These post-drive plasmas persist for several milliseconds, obey radial force balance, and can be routinely reconstructed with the magnetic equilibrium code. Line-integrated density measurements indicate good particle confinement, and both measured soft x-ray spectra and oxygen emission line ratios suggest an increasing electron temperature. Fast-frame visible-wavelength imaging shows sharp, bright plasma edges which match typical highly shaped low-aspect-ratio tokamaks.

The long decay time of gun-initiated plasmas is well suited for hand off to other current drive systems, including inductive drive from the central solenoid. In Fig. 3, an 80 kA gun-driven discharge is handed off to inductive drive, reaching $I_p > 150$ kA using only 18 mV s of inductive flux from the central solenoid. Approximately 36 mV s is required to produce a similar discharge using inductive drive only. After handoff, the plasma parameters are consistent with typical tokamak operations. This compatibility with inductive current drive after gun shutoff demonstrates that the decaying plasma has closed flux surfaces with good confinement.

The maximum I_p that can be formed and sustained using point-source dc helicity injection is constrained by helicity balance and Taylor relaxation. The helicity injection rate ($\dot{K}_{dc}$) from the biased plasma guns can be expressed as an effective loop voltage [2]:

$$V_{\rm eff} \approx \frac{B_{\phi 0}}{\langle B_\phi \rangle} \frac{R_0}{A_p} \frac{\pi N_{\rm gun} D_{\rm gun}^2}{4 R_{\rm gun}} V_{\rm bias}. \quad (1)$$

Here, $B_{\phi 0}$ is the vacuum toroidal field at R_0, $\langle B_\phi \rangle$ is the volume-averaged toroidal field, A_p is the cross-sectional area of the plasma, $D_{\rm gun}$ is the diameter of the plasma gun arc, and $N_{\rm gun}$ and $R_{\rm gun}$ are, respectively, the number and major radius of identical plasma guns. Helicity is also injected via an inductive loop voltage ($V_{\rm ind}$) due to the increasing vertical field required to maintain radial force balance. In steady state, the helicity injection rate equals

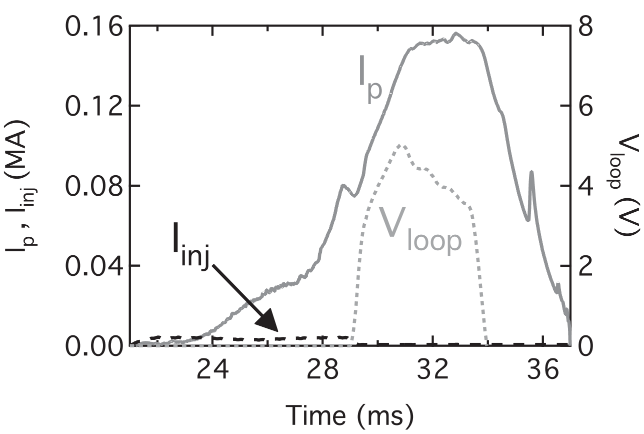

FIG. 3. Inductive drive from the central solenoid is applied during the decay of an 80 kA gun-produced discharge.

resistive dissipation, giving $I_p \leq A_p(V_{\rm eff} + V_{\rm ind})/2\pi R_0 \langle \eta \rangle$, where $\langle \eta \rangle$ is the volume-averaged plasma resistivity.

Taylor relaxation also constrains I_p by limiting the magnetic inverse scale length λ ($\lambda = \mu_0 J_\parallel / B$) in the gun-driven plasma. As postulated by Taylor [1], an edge-driven discharge will relax via magnetic turbulence toward the lowest-energy, force-free topology (governed by $\nabla \times \mathbf{B} = \lambda \mathbf{B}$), where λ is a constant throughout. If the helicity injection scheme sets an average edge λ value ($\bar{\lambda}_{\rm edge}$), then relaxation imposes a maximum value on I_p ($\lambda_p \leq \bar{\lambda}_{\rm edge}$, where $\lambda_p = \mu_0 I_p / A_p \langle B_\phi \rangle$) [14].

While the current injection at the plasma edge due to a local current source is inherently nonaxisymmetric, turbulent mixing and magnetic shear effectively distribute the injected current throughout the entire edge region. High-speed imaging of Pegasus discharges shows the discrete current filaments rapidly becoming diffuse and indistinct within the edge region. Likewise, experiments on the SSPX spheromak demonstrated that a nonaxisymmetric λ distribution near coaxial electrodes was effectively averaged over the plasma edge [15]. As a first-order estimate, it is thus reasonable to take $\lambda_{\rm edge}$ to be approximately uniform in the plasma edge region.

With this assumption, the average edge λ is given by $\bar{\lambda}_{\rm edge} = \mu_0 I_{\rm inj} / \psi_{\rm edge}$ for a current $I_{\rm inj}$ flowing in an axisymmetric sheet of poloidal flux of radial width w between the guns and anode at radius $R_{\rm gun}$. The relaxation limit, $\lambda_p \leq \bar{\lambda}_{\rm edge}$, then gives the upper limit to I_p as

$$I_p \leq f_G \left[\frac{\varepsilon A_p I_{\rm TF} I_{\rm inj}}{2\pi R_{\rm gun} w} \right]^{1/2}, \quad (2)$$

where f_G is a dimensionless function that accounts for a finite aspect ratio and noncircular cross section. In full-size Pegasus discharges, $f_G \sim 3$, and approaches unity for large-A, circular cross section plasmas.

The relaxation limit determines the maximum achievable I_p, assuming sufficient helicity injection is provided. If there is insufficient helicity injection (i.e., relatively low $V_{\rm eff}$), then the sustained I_p will be below this relaxation limit. This is supported experimentally by data shown in Fig. 4, where I_p is plotted versus R_0 for three discharges with different helicity injection rates and compared to the calculated relaxation limit. The relaxation limit is estimated using a plasma geometry evolution that begins as a circular cross section, high aspect ratio plasma at large R_0 and ends as the highly shaped, low-aspect-ratio geometry shown in Fig. 2. The rapid increase in the relaxation limit as R_0 decreases is predominately due to increases in the inverse aspect ratio, the plasma cross-sectional area, and f_G as the plasma moves inward and becomes more highly shaped.

For the three discharges shown in Fig. 4, $V_{\rm bias}$ (and hence, $V_{\rm eff}$) is varied by changing the neutral fueling rate in the plasma guns with all other operational parameters

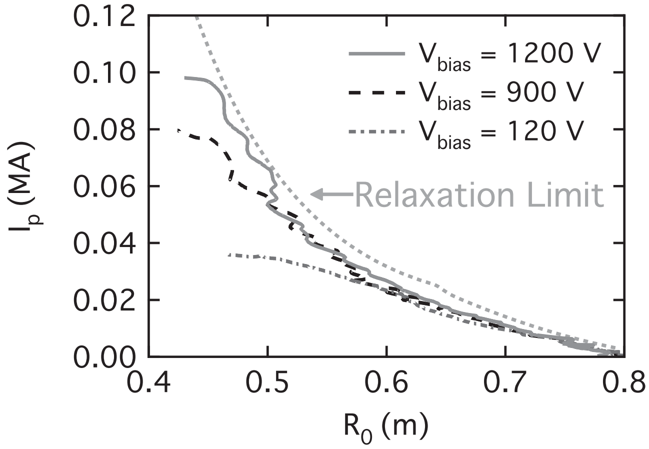

FIG. 4. I_p versus R_0 for three discharges with different V_{bias} compared to limit estimated from Eq. (2).

fixed. The trajectory for the discharges follows the estimated relaxation limit until the I_p limit determined by helicity balance is reached. For the lower two trajectories, the helicity injection rate is not sufficient to drive the plasma current to the maximum I_p allowed by the relaxation limit.

These first results qualitatively agree with the simple model invoking helicity balance and magnetic relaxation, with the assumption that the effective $\bar{\lambda}_{\mathrm{edge}}$ can be approximated by uniformly distributing the injected current in the plasma edge. The development of a predictive model for future applications requires additional study to directly investigate the mechanisms that influence $\bar{\lambda}_{\mathrm{edge}}$ and determine the injector impedance. The degree of stochasticity of the magnetic field and its relationship to energy confinement, plasma temperature, and resistivity, and their respective dependencies on the helicity drive, also require further study.

These results complement earlier experiments on Pegasus at lower I_p, where two plasma guns were mounted near the inboard edge of the lower divertor plate region [16], and together they demonstrate the geometric flexibility of the technique. With appropriate high-current density sources, helicity injection via local current sources in the plasma periphery may provide a viable and flexible approach for starting up and driving currents in tokamaks and other magnetically confined toroidal plasmas.

The authors thank E. Hinson, J. Cole, A. Robinson, and A. Wiersma for their assistance with Pegasus operations and G. Winz, B. Lewicki, and B. Kujak-Ford for the design and construction of the plasma gun system. This work is supported by U.S. DOE Grant DE-FG02-96ER54375.

[1] J. Taylor, Rev. Mod. Phys. **58**, 741 (1986).
[2] M. Ono, G. J. Greene, D. Darrow, C. Forest, H. Park, and T. H. Stix, Phys. Rev. Lett. **59**, 2165 (1987).
[3] D. Darrow *et al.*, Phys. Fluids B **2**, 1415 (1990).
[4] T. Jarboe, Plasma Phys. Controlled Fusion **36**, 945 (1994).
[5] A. Redd, T. Jarboe, W. Hamp, B. Nelson, R. O'Neill, and R. Smith, Phys. Plasmas **15**, 022506 (2008).
[6] R. Raman *et al.*, Nucl. Fusion **41**, 1081 (2001).
[7] G. Garstka *et al.*, Nucl. Fusion **46**, S603 (2006).
[8] A. Redd, D. Battaglia, M. Bongard, R. Fonck, E. Hinson, B. Kujak-Ford, B. Lewicki, A. Sontag, and G. Winz, J. Fusion Energy **28**, 203 (2009).
[9] G. Fiksel, A. F. Almagri, D. Craig, M. Iida, S. C. Prager, and J. S. Sarff, Plasma Sources Sci. Technol. **5**, 78 (1996).
[10] D. Den Hartog, D. Craig, G. Fiksel, and J. Sarff, Plasma Sources Sci. Technol. **6**, 492 (1997).
[11] D. Battaglia, M. Bongard, R. Fonck, A. Redd, and A. Sontag, J. Fusion Energy **28**, 140 (2009).
[12] C. Sovinec, B. Cohen, G. Cone, E. Hooper, and H. McLean, Phys. Rev. Lett. **94**, 035003 (2005).
[13] A. Sontag, S. Diem, R. Fonck, G. Garstka, E. Unterberg, and T. Thorson, Nucl. Fusion **48**, 095006 (2008).
[14] B. Nelson, T. Jarboe, D. Orvis, L. McCullough, J. Xie, C. Zhang, and L. Zhou, Phys. Rev. Lett. **72**, 3666 (1994).
[15] C. Holcomb, T. Jarboe, D. Hill, S. Woodruff, and R. Wood, Phys. Plasmas **13**, 022504 (2006).
[16] N. Eidietis, R. Fonck, G. Garstka, E. Unterberg, and G. Winz, J. Fusion Energy **26**, 43 (2007).